

Time-Resolved Unimolecular Fragmentations of $C_3H_7O^+$ Ions

Ryuichi ARAKAWA* and Yozaburo YOSHIKAWA

Institute of Chemistry, College of General Education, Osaka University, Osaka 560

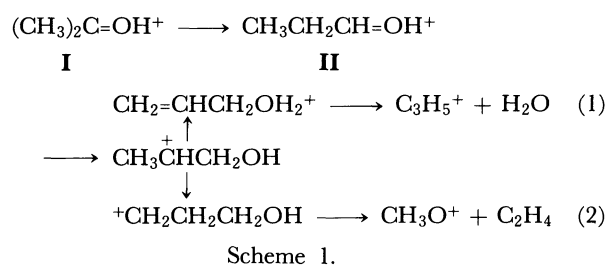
(Received December 26, 1986)

The unimolecular dissociations of the $C_3H_7O^+$ ions produced by the dissociative ionization of *t*-butyl and *s*-butyl alcohols have been studied by means of trapped ion mass spectrometry (TIMS). The metastable peak intensities for two competing formations of $C_3H_5^+$ and CH_3O^+ have been measured for the ion lifetimes of 0–50 μ s. Also, the shifts of the electron-ionization-efficiency (EIE) curves for these ions have been observed between the ion-storage times of 2 and 800 μ s. These data have then been fitted by means of QET model calculations. The dissociation paths of $C_3H_7O^+$ can be interpreted without any assumption of a rate-determining isomerization process.

The potential energy profiles have been of much interest in understanding the reaction mechanism. One of the problems is the experimental uncertainty concerning a rate-determining isomerization process or its barrier height on the potential surface. In a $C_3H_7O^+$ system, most of the studies have employed electron-impact (EI) ionization,^{1–5)} isotope labeling techniques,^{6,7)} and chemical ionization (CI)^{8,9)} for metastable fragmentations. Collision-induced dissociation (CID) spectra of ions have been used for the identification of ion structures.¹⁰⁾ The molecular orbital calculations¹¹⁾ have provided accurate knowledge about the relative energies of the various $C_3H_7O^+$ ions involved on the potential energy surface. In the reaction paths for water and ethylene elimination (Scheme 1), several structures of $C_3H_7O^+$ ions have been postulated to lie on the same potential energy surface. Detailed potential energy surfaces for the fragmentations of $(CH_3)_2C=OH^+$ [I] and $CH_3CH_2CH=OH^+$ [II] have been studied by Williams and his co-workers.^{2,3)} Their results for the ratios of the metastable peak intensity or kinetic energy releases showed that the fragmentation of I by either reaction, 1 or 2, involves a rate-determining isomerization to II prior to fragmentation. Harrison et al.⁹⁾ have obtained the same conclusion from the fact that the ratios of metastable peak intensities for I are essentially insensitive to activation modes, such as the EI, CI, and CID methods. However, measurements of the metastable appearance energies for $C_3H_5^+$ and CH_3O^+ with energy-selected electrons have shown that the fragmentations of the I and II isomers, which were formed from *t*-butyl and *s*-butyl alcohols respectively, take place at the thermochemical threshold.⁴⁾

There is no consistent explanation for the rate-determining isomerization of I \rightarrow II. Therefore, our present study examines in more detail the fragmentations of the I and II ions by means of time-resolved measurements of the metastable peak intensities and the EIE curves. In particular, an experiment for long-lifetime ions can study the lower internal energy fragmentation than have previous studies. A wide variation in ion lifetimes permits a close comparison of the metastable peak intensity with the calculated inten-

sity by assuming the rate models. The TIMS experiment can change the ion residence time up to several milliseconds, so that the unimolecular reaction of 10^3 – 10^6 s^{–1} can be sampled.



Experimental

The ion-trapping technique has been described in detail elsewhere.¹²⁾ The space charge formed by a continuous 5-eV electron beam was used to trap ions produced when a negative pulse was applied to a filament. At a known delay time after the ionizing pulse, a positive pulse 5 μ s in duration and 4 eV high was applied to a repeller electrode in order to remove ions for mass analysis. Argon ions were stored far up to several milliseconds without any serious decrease in the trapped ion concentration, as is shown in Fig. 1. An ionizing pulse 2 μ s in duration was applied to the filament at 1 ms-intervals. The nominal electron energy was varied by changing the pulse height applied to the filament.

A home-built tandem-type mass spectrometer was used to measure the EIE curves and the metastable fragmentation. The parent ions, which are selected by the first magnet,

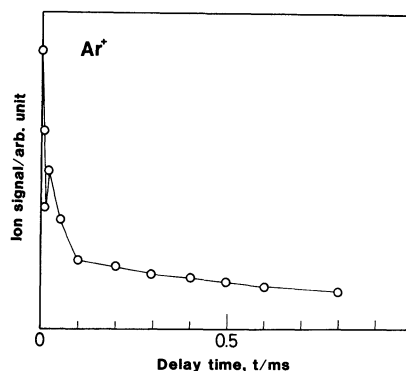


Fig. 1. Argon ion signals as a function of the delay time, *t*.

decompose in the second field free region between two magnets. The product ions are analyzed by the second magnet. A data accumulation of about an hour was statistically needed for both the EIE and metastable peak measurements. The temperature of the ion source was 423 K. The ion-accelerating voltage was 1.5 kV. The ion-source pressure was kept at 2×10^{-6} Torr (1 Torr = 133.32 Pa). The collision-induced reactions were negligible, because the pressure in the field free region was always less than 1×10^{-6} Torr. Samples were commercially obtained.

Results and Discussion

Figure 2 shows the time-resolved EIE curves for the $C_3H_5^+$ and CH_3O^+ fragments produced from *t*-butyl and *s*-butyl alcohols. The argon EIE curve was used for the EIE curve normalization between different ion

storage times, because the ion trapping efficiency decreases with the delay time, as is shown in Fig. 1. The EIE shifts observed at $V=13.5$ eV are about 0.4 eV for $C_3H_5^+$ and zero for CH_3O^+ . These shifts are due to the so-called "kinetic shift," the excess energy required to produce a detectable dissociation (usually 10^5 s $^{-1}$) of a polyatomic ion. The molecular ions for both samples were very low in intensity in the present energy range, while the $C_3H_7O^+$ fragment is very abundant on both mass spectra. The EIE shifts with the delay times are, therefore, believed to be caused by the slow dissociation, not for the molecular ions, but for the $C_3H_7O^+$ precursor ions.

The time-dependent EIE for the *i*-th daughter ion at a nominal electron energy V can be written in this form:¹³⁾

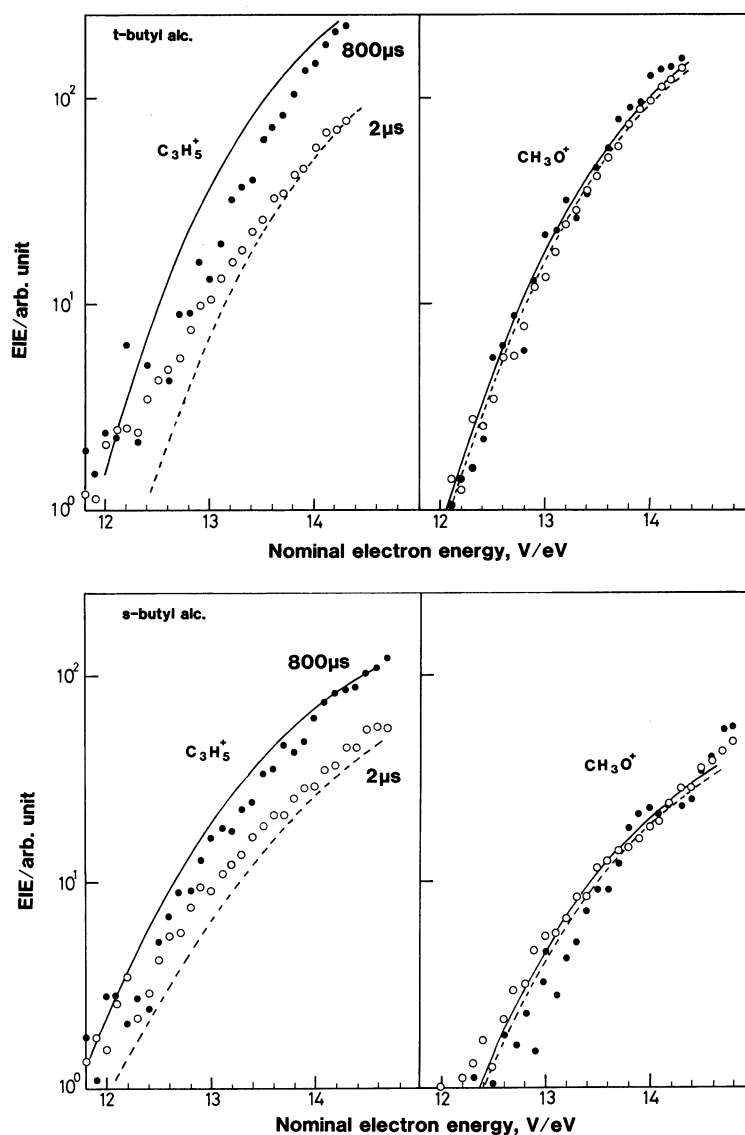


Fig. 2. Time-resolved electron-ionization-efficiency (EIE) curves for $C_3H_5^+$ and CH_3O^+ daughter ions vs. nominal electron energy V : (a) *t*-butyl alcohol, (b) *s*-butyl alcohol. ● (—) and ○ (---) indicate the experimental (calculated) EIEs of $t=800$ and 2 μ s, respectively.

$$EIE_i(V,t) \propto \int_0^\infty m(E'-V) \left[\int_{AE_0}^{E'} f(E',E) \times \right. \\ \left. (k_i(E)/\sum k_j(E)) w(E) dE \right] dE' \quad (3),$$

where t is the ion-source-residence time, $m(E'-V)$ is the instrumental electron-energy distribution, E' is the total electron energy, $f(E',E)$ is the internal energy distribution of $C_3H_7O^+$, AE_0 is the 0 K appearance energy for the daughter ion, $k_i(E)$ is the unimolecular rate constant for the i -th path, and $w(E)$ is the fraction of dissociation given by $1 - \exp(-t \sum k_j(E))$. The $m(E'-V)$ distribution was obtained from the second derivatives of a helium experimental EIE curve on the basis of Morrison's method¹⁴; its half-width was 0.8 eV. The $f(E',E)$ distribution for the ionized $C_3H_7O^+$ was assumed to be equal to that for the molecular ions. From the ionization-threshold law,¹⁵ the energy distribution for molecular ions can be given by $p(E)(E'-E)$, where $p(E)$ is the energy-deposition function. The photoelectron spectra of *t*-butyl and *s*-butyl alcohols were assumed to represent $p(E)$.¹⁶

The decay rates were obtained from a simple form¹⁷ of $k(E) = \nu(1 - E_0/E)^s$, where ν is the frequency factor, E_0 is the activation energy, and s is the effective number of oscillators. In the same reaction system, Tsang and Harrison¹¹ have investigated, by means of model calculation, the effect of change in the internal energy distribution on the metastable peak ratio of $C_3H_5^+/CH_3O^+$. Their adjusted parameters of the frequency factor were $\nu_a = 10^{8-9}$ and $\nu_b = 10^{11-10^{12}}$ for reactions 1 and 2 respectively. In the present calculation, we employed similar parameters of the frequency factor, as are summarized in Table 1. Moreover, for the sake of simplicity, the frequency factors for **I** and **II** were assumed to be the same. The s value was taken to be 9, corresponding to a third of the number of vibrational degrees of freedom of $C_3H_7O^+$. The activation energies were obtained from the potential energy diagram illustrated in Ref. 9, assuming that the dissociations occur at their thermochemical onsets. The calculated EIE curves are in fair agreement with the experimental curves. The amount of the EIE shift between different delay times depends principally on the rising steepness of the $k(E)$ vs. E curves. As may be seen in Fig. 2, the EIE shift is greater for $C_3H_5^+$ formation than for CH_3O^+ . This is because the $k(E)$ curve of $C_3H_5^+$, having the smaller frequency factor, rises more slowly with the energy.

The metastable peak intensities relative to the parent ions, $m^*/C_3H_7O^+$, for the **I** and **II** ions are shown in Fig. 3 for the range of $t=0-50 \mu s$. Our ratios of the peak intensities, $C_3H_5^+/CH_3O^+$, at $t=0 \mu s$ agree with those of the literature.⁹ The experimental errors estimated were, at most, 20%. After a careful consideration of the reproducibility and error limits, we obtained the significant result for **I** that the peak intensities between $C_3H_5^+$ and CH_3O^+ are reversed at a long delay time. This result is inconsis-

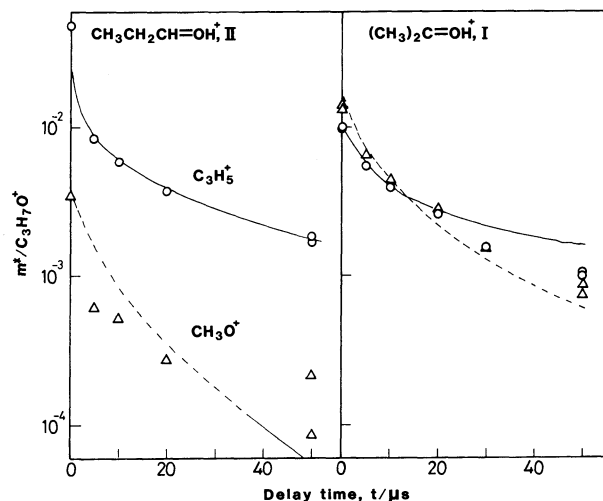


Fig. 3. A plot of metastable peak intensities relative to the parent ion, $m^*/C_3H_7O^+$, against delay time when $V=40$ eV. Experimental (calculated) data; $C_3H_5^+$, \circ (—) and CH_3O^+ , Δ (---). The ions **I** and **II** were produced by dissociative ionization from *t*-butyl and *s*-butyl alcohols, respectively.

ent with the previous results^{3,9} indicating that the metastable peak ratios are insensitive to ion formation and to ion lifetime of several microseconds. Its lifetime was varied by change in an accelerating voltage. The ratios of $C_3H_5^+/CH_3O^+$ are not affected by the ion lifetime if there is the rate-determining isomerization of **I**→**II**. The metastable peak intensities were calculated assuming the direct fragmentation of **I** and **II** to products. For the calculation, Eq. 3 was modified in such a way that $w(E)$ was replaced by $\exp(-t_1 \sum k_j(E)) - \exp(-t_2 \sum k_j(E))$. Therefore, $w(E)$ means the fraction of dissociation occurring in the second field-free region. t_1 and t_2 are the entrance and exit times relative to the time of ion formation ($t_1 = 5.8 + t$ and $t_2 = 10.1 + t \mu s$).

The smooth lines in Fig. 3 are the fragmentation curves calculated by the use of the same rate models as in Table 1. The overall agreement with the experimental curves is fairly satisfactory. The rate-determining isomerization of **I**→**II** was supported by the experimental evidence that the metastable-peak ratios for **I** were independent of the activation modes. In other words, the relative rates were essentially constant over the internal-energy range generated. Accordingly, the rate-determining isomerization mechanism may be ruled out by the presence of curve crossing for **I**.

Table 1. Activation Energies and Frequency Factors Used in the Rate Model of the $C_3H_7O^+$ Dissociation

Ion	$C_3H_5^+$		CH_3O^+	
	E_0	ν_a	E_0	ν_b
	eV	s ⁻¹	eV	s ⁻¹
I	2.08	$10^{8.5}$	2.66	10^{11}
II	1.56	$10^{8.5}$	2.14	10^{11}

A collisional deactivation and an infrared radiative decay are nondissociative processes particularly important for long-lived ions. However, these processes proved to have no effect on the EIE curves or the metastable fragmentations at the present pressure of the sample. This has previously been discussed in detail in the case of pyridine dissociation.¹³⁾

The time-resolved measurements of EIEs and metastable fragmentations lead to the conclusion that the dissociations of **I** and **II** require no hypothesis of the rate-determining isomerization or the barrier on their paths. This conclusion is exclusively valid for the dissociation of ions whose internal energy is close to the threshold. In the case of $t=50\ \mu\text{s}$, for example, the rate of $k(E)=1.7\times 10^4\ \text{s}^{-1}$ corresponding to a peak of $w(E)$ contributes principally to metastable fragmentation.

References

- 1) C. W. Tsang and A. G. Harrison, *Org. Mass Spectrom.*, **7**, 1377 (1973).
- 2) G. Hvistendahl, R. D. Bowen, and D. H. Williams, *J. Chem. Soc., Chem. Commun.*, **1976**, 294.
- 3) R. D. Bowen, J. R. Kalman, and D. H. Williams, *J. Am. Chem. Soc.*, **99**, 5481 (1977); R. D. Bowen, D. H. Williams, G. Hvistendahl, and J. R. Kalman, *Org. Mass Spectrom.*, **13**, 721 (1978).
- 4) J. L. Holmes and J. K. Terlouw, *Org. Mass Spectrom.*, **15**, 383 (1980).
- 5) G. Hvistendahl and D. H. Williams, *J. Am. Chem. Soc.*, **97**, 3097 (1975).
- 6) C. W. Tsang and A. G. Harrison, *Org. Mass Spectrom.*, **5**, 877 (1971).
- 7) J. H. Holmes, R. T. B. Rye, and J. K. Terlouw, *Org. Mass Spectrom.*, **14**, 606 (1979).
- 8) R. D. Bowen and A. G. Harrison, *Org. Mass Spectrom.*, **16**, 159 (1981).
- 9) A. G. Harrison, T. Gaumann, and D. Stahl, *Org. Mass Spectrom.*, **18**, 517 (1983).
- 10) F. W. McLafferty and I. Sakai, *Org. Mass Spectrom.*, **7**, 971 (1973).
- 11) R. H. Nobes and L. Radom, *Org. Mass Spectrom.*, **19**, 385 (1984).
- 12) A. A. Herod and A. G. Harrison, *Int. J. Mass Spectrom. Ion Phys.*, **4**, 415 (1970); C. Lifshitz, *Mass Spectrom. Rev.*, **1**, 309 (1982).
- 13) R. Arakawa and Y. Yoshikawa, *Bull. Chem. Soc. Jpn.*, **60**, 49 (1987).
- 14) J. D. Morrison, *J. Chem. Phys.*, **21**, 1767 (1953).
- 15) M. R. H. Rudge, *Rev. Mod. Phys.*, **40**, 564 (1968); M. R. H. Rudge and M. J. Seaton, *Proc. Phys. Soc.*, **83**, 680 (1964).
- 16) A. D. Baker, D. Betteridge, N. R. Kemp, and R. E. Kirby, *Anal. Chem.*, **43**, 375 (1971).
- 17) H. M. Rosenstock, M. B. Wallenstein, A. L. Wahrhaftig, and H. Eyring, *Proc. Natl. Acad. Sci. U.S.A.*, **38**, 667 (1952).